

Excited State Structure and Dynamics of *p*-Benzoquinone and Bromanil from Time-Resolved Resonance Raman Spectra and Simulation

Mrinalini Puranik[#] and Siva Umapathy[*,##]

Department of Inorganic and Physical Chemistry, Indian Institute of Science, Bangalore-560012, India

(Received October 1, 2001)

p-Benzoquinone and its halogen substituted derivatives are known to have differing reactivities in the triplet excited state. While bromanil catalyzes the reduction of octaethylporphyrin most efficiently among the halogenated *p*-benzoquinones, the reaction does not take place in presence of the unsubstituted *p*-benzoquinone (T. Nakano and Y. Mori, *Bull. Chem. Soc. Jpn.*, **67,** 2627 (1994)). Understanding of such differences requires a detailed knowledge of the triplet state structures, normal mode compositions and excited state dynamics. In this paper, we apply a recently presented scheme (M. Puranik, S. Umapathy, J. G. Snijders, and J. Chandrasekhar, *J. Chem. Phys.*, **115,** 6106 (2001)) that combines parameters from experiment and computation in a wave packet dynamics simulation to the triplet states of *p*-benzoquinone and bromanil. The absorption and resonance Raman spectra of both the molecules have been simulated. The normal mode compositions and mode specific excited state displacements have been presented and compared. Time-dependent evolution of the absorption and Raman overlaps for all the observed modes has been discussed in detail. In *p*-benzoquinone, the initial dynamics is along the C=C stretching and C–H bending modes whereas in bromanil nearly equal displacements are observed along all the stretching coordinates.

Most photochemical reactions involve the creation of excited states which either react themselves or form other short-lived reactive species like neutral, anionic and cationic radicals. A molecule in the singlet ground state typically forms the excited singlet state on absorption of light, which may relax by many ways. One of the possibilities is intersystem crossing to form the triplet excited state. Since transition from the triplet excited state to the ground state is forbidden, it has longer lifetime than the singlet excited state and therefore facilitates excited state reactions better than singlet state reactions. Hence, the reactivities of triplet excited states are of considerable interest.

Quanititative understanding of the reactivities of the triplet states necessarily requires detailed knowledge of their structures. One of the means of obtaining structural information of short-lived states is time-resolved resonance Raman spectroscopy. The technique offers the advantages of selectivity and sensitivity. Kinetics of individual intermediates can be monitored in the presence of several species by tuning the excitation wavelength. The positions of the observed bands in the vibrational spectra are interpreted to obtain structural information of the species of interest. However, a lot of information is also contained in the intensities of the observed spectral bands which is not utilized in a quantitative way. In contrast, in the ground state, the theory of resonance Raman intensities developed by Lee and Heller[1] has been successfully applied for a large number of systems and has been reviewed extensively.[2–7] The commonly used approaches have been to either obtain parameters from experiments and fit them to reproduce experimental intensities[2–13] or to use ab initio calculations to predict the spectra.[14–17] In the former method, mode specific displacements of the excited state potential energy surface are extracted from the empirical data where as in the latter method, one is more likely to assess the accuracy of the methods used to predict the spectra.

One of the problems in the extension of the purely empirical method to short-lived intermediates is that the separation of the ground state of the species of interest and its resonant excited state and the oscillator strength of the transition cannot be determined without additional experiments. In the stable, ground state molecules, this energy may be estimated from the knowledge of the absorption and fluorescence spectra. Resonance Raman intensities of transient states have been theoretically estimated by Wilbrandt and coworkers,[16,17] e. g., in the radical cations of 1, 3, 5-hexatriene, triphenylene, *N*, *N*-dimethylpiperazine and *N*,*N*-dimethylaniline, triplet states of 1, 3, 5-hexatriene, 2, 5-dimethy1-1, 3, 5,-hexatriene and stilbene and by Hudson and coworkers[14,15] in imidazole, imidazolium and their derivatives, *N*-methylacetamide, etc., successfully. However, computation of transient state resonance Raman spectra from purely quantum mechanical calculations is an involved process and requires high level calculations which often are time consuming and expensive, especially for large polyatomic systems.

Recent work has demonstrated that density functional theory is a reliable and accurate method for the prediction of vibrational spectra of ground and excited state molecules.[18–25] The development of time-dependent density functional theory has made it possible to compute singlet–singlet and singlet–triplet excitation energies with a reasonable amount of computational

Department of Organic Chemistry, Indian Institute of Science, Bangalore-560012, India
Swarnajayanti Fellow.

effort.[26,27] Therefore, many groups, including us, have been involved in a systematic assessment of the performance of these methods for several molecules, especially quinones.

We have recently presented a scheme in which parameters from time-resolved resonance Raman experiments, density functional theory and time-dependent density functional theory were utilized in a wave packet dynamics simulation of the resonance Raman intensities.[25] The simulations of the triplet state of bromanil yielded valuable information on the resonant triplet state. Modeled spectra were used to assign the observed $T_1 \rightarrow T_n$ transition and to obtain mode-specific displacements of the excited triplet state potential energy surface with respect to the lowest triplet state surface. The geometry of the T_n state predicted from the simulated dimensionless displacements was in agreement with DFT calculated geometry. In this paper, we have applied the above technique to the triplet state spectra of the parent benzoquinone along with bromanil in order to understand the influence of substitution on the structure and dynamics. The resonance Raman and absorption spectra, normal modes and excited state dimensionless displacements of the parent and substituted benzoquinone have been compared. The initial mode-specific dynamics has been discussed in detail. Knowledge of the initial dynamics and the mode-specific excited state displacements of the two quinones have yielded insight into differing reactivities of the parent and substituted quinone.

Experimental Methods

Experimental methods and procedures used for the TR3 spectroscopy have been described previously.[28] Briefly, the pump beam is the third harmonic output of a 1064 nm fundamental from an Nd:YAG laser (DCR 11, Spectra Physics). The probe beam is obtained from an optical parametric oscillator (OPO) which is pumped by the third harmonic of 1064 nm output from an Nd: YAG laser (GCR 250, Spectra Physics). The probe wavelength 512 nm was obtained from the OPO. The pulses had typical energies of 2.5 mJ and were ca. 10 ns in temporal width for both pump and probe lasers. The scattered light was dispersed using a SPEX double monochromator with two 600 groves/mm gratings. The multichannel detector used was a liquid Nitrogen cooled CCD from Princeton Instruments with 576×378 pixels. The spectra have been calibrated using known solvent bands as reference and the spectral resolution has been estimated as 5 cm^{-1}. The concentration used for the Raman experiments was ca. 2 mM (1 M = 1 mol dm^{-3}).

Bromanil used was purchased from Aldrich Chemicals. Both, bromanil and the solvents were of analytical grade and used without further purification. Sample solutions were circulated through a capillary at a rate of about 10 mL per minute to avoid possible accumulation of photoproducts. The probe only spectra were recorded periodically to confirm the absence of photoproducts.

Theory and Computational Methods

Density functional theoretical calculations were performed with the Amsterdam Density Functional (ADF99) package[29] on a cluster of IBM RS 6000/43P workstations. Calculations for the triplet excited state used the unrestricted formalism. The basis set used was TZP (Basis IV in ADF terminology) that is a part of the ADF program.[29] The singlet–triplet excitation energies and the transition dipole lengths were computed using TDDFT as implemented in the Response[26] code in the ADF packege of programs. Density functional calculations involved the Local Density approximation of Vosko, Wilk and Nussair (VWN),[30] gradient corrected exchange functional proposed by Becke[31] and the correlation functional of Lee, Yang and Parr.[32] Normal mode analysis was carried out using NMODES,[20] a program developed in our laboratory which used the normal mode eigen vectors computed using the ADF package to compute the potential energy distribution. Wave packet dynamical simulations were carried out using MATLAB on an IBM RS 6000 workstation using the analytical solutions mentioned below. The Fourier transform and inverse Fourier transform routines used were a part of the MATLAB library. Time step used for the simulation was 0.01 fs.

The time-dependent theory of Lee and Heller[1] for resonance Raman scattering has been used to simulate the observed absorption and the relative Raman intensities. In this approach, the energy denominator of the sum-over-states expression of the Raman polarizability in Eq. 1

$$\alpha_{if}(E_L) = M^2 \sum_{v} \frac{\langle f|v\rangle\langle v|i\rangle}{\varepsilon_v - \varepsilon_i + E_0 - E_L - i\Gamma} \tag{1}$$

is written in the form of an integral over a time variable.[1] If all the PESs are assumed to be harmonic and separable, we obtain the following expression for the Raman cross section it the time-domain,[1,33]

$$\sigma_{i\rightarrow f}(E_L) = \frac{8\pi E_s^3 E_L e^4 M^4}{9\hbar^6 c^4} \left| \int_0^\infty \langle f|i(t)\rangle \exp[i(E_L + E_i)t/\hbar - \frac{\Gamma t}{\hbar} - \frac{\theta^2 t^2}{2\hbar}] dt \right|^2, \tag{2}$$

and the corresponding expression for the absorption spectrum is given by,

$$\sigma_A(E_L) = \frac{4\pi e^2 M^2 E_L}{6\hbar^2 c} \int_{-\infty}^{\infty} \langle i|i(t)\rangle \exp[i(E_L + E_i)t/\hbar - \frac{\Gamma|t|}{\hbar} - \frac{\theta^2 t^2}{2\hbar}] dt. \tag{3}$$

Here, $|i(t)\rangle$ denotes the wave packet evolving on the resonant excited state surface (RES) at various intervals of time (t), under the influence of excited state vibrational Hamiltonian, H_{ex} given by the following expression:

$$|i(t)\rangle = \exp\left(-\frac{iH_{\mathrm{ex}}t}{\hbar}\right)|i\rangle \tag{4}$$

where, $\exp(-iH_{\mathrm{ex}}t/\hbar)$ is the time evolution operator. The incident and scattered photon energies are E_{L} and E_{s}, E_{i} is the zero-point vibrational energy of the T_1 state, M is the electronic transition dipole length evaluated at the equilibrium geometry of the T_1 state for the transition from the T_1 state to the resonant excited state (RES), T_{n}, e is the electronic charge and c is the velocity of light. Motion of the time-evolving wave packet on the excited state is damped by two terms, $\exp(-\Gamma t/\hbar)$ and $\exp(-\theta 2t2/2\hbar)$ which include broadening due to finite lifetime (Γ) as well as that induced by solvent (θ).

The system is initially in a state $|i\rangle$, which is a vibrational eigen state of the lower triplet state (T_1) surface. Interaction with the incident light transports the wave packed to the excit-

ed state. Since the wave packet is not an eigen state of the excited state Hamiltonian, it begins to evolve in time and is denoted by $|i(t)\rangle$. The absorption and Raman cross sections are obtained by talking the overlap of this time-evolving wave function with the ground vibrational state of the T_1 state, $|0\rangle$ (for absorption) and the first excited vibrational state of T_1, $|1\rangle$ (for Raman).

If we assume that the vibrational potential energy surfaces are harmonic, separable and that the frequencies of the ground and excited state are identical, i. e., there is no Duschinski rotation, the expressions for the absorption and Raman cross sections are considerably simplified and are given by.[4]

$$\sigma_A(E_L) = \frac{4\pi e^2 M^2}{6\hbar^2 c} \int_{-\infty}^{\infty} \exp\left[i(E_L - E_0)t/\hbar - \Gamma|t|/\hbar - \frac{\theta^2 t^2}{2\hbar} \right] \cdot \prod_{j=1}^{N} \exp\left\{ -\frac{\Delta_j^2}{2}\left[1 - \exp^{-i\omega_j t}\right] \right\} dt \quad (5)$$

and

$$\sigma_{i\to f}(E_L) = \frac{8\pi e^4 M^4 E_S^3 E_L}{9\hbar^6 c^4} \left| \int_0^{\infty} \exp\left[\begin{matrix} i(E_L - E_0)t/\hbar \\ -\Gamma|t|/\hbar - \dfrac{\theta^2 t^2}{2\hbar} \end{matrix} \right] \cdot \frac{\Delta_1}{\sqrt{2}}(e^{-i\omega_1 t} - 1) \prod_{j=1}^{N} \exp\left\{ -\frac{\Delta_j^2}{2}\left[1 - \exp^{-i\omega_j t}\right] \right\} dt \right|^2, \quad (6)$$

where, E_0 is the separation between the zero-point energies of the T_1 and T_n states and Δ_j denotes the relative dimensionless displacements between the PESs of the T_1 and T_n states along the jth mode. Therefore the parameters required for the simulation of the resonance Raman spectrum are the zero-zero energy (E_0), the transition dipole length for the $T_1 \rightarrow T_n$ transition, guess values for the displacements (Δ_j) and vibrational frequencies (ω_j) of the observed normal modes. In the following we discuss each of these parameters along with the procedures used to obtain initial guesses in detail.

Detailed dicdussion on individual parameters have been given recently.[25] Briefly, a DFT calculation was carried out to obtain the optimized geometry of the ground state (S_0) for each of the systems. That the obtained geometry is a minimum was confirmed by computing the vibrational frequencies (no imaginary frequencies). At this geometry, the singlet–singlet and singlet–triplet excitations were computed using TDDFT. The lowest triplet state was identified and the geometry was optimized for the T_1 state and vibrational frequencies were computed. At this triplet state geometry, the singlet-triplet excitations were recomputed. The excitation energies were analyzed and the resonant triplet state was identified by comparison with the observed maximum in the $T_1 \rightarrow T_n$ transient absorption spectrum. This is defined as the difference in energies:

$$\Delta E(T_1 \rightarrow T_n) = E(S_{\text{trip.geom}} \rightarrow T_1) - E(S_{\text{trip.geom}} \rightarrow T_n). \quad (7)$$

The guess displacements for the simulation are calculated from the ratios of relative intensities of the observed Raman spectra using the approximation $I_j \propto \Delta_j^2 \omega_j^2$.[34] The broadening parameters were guessed and changed iteratively to obtain the best fit. We note however, that the absorption spectrum alone is not sensitive to the partitioning of homogeneous and inhomogeneous broadening parameters. For the unique determination of these parameters, simultaneous fitting of all the Raman excitation profiles and the absorption spectrum is necessary.

Results and Discussion

Most phenyl ketones have n–π^* and π–π^* states with comparable energy and this is also the case with quinones. The lowest triplet state in p-benzoquinone is accepted to be the $^3B_{1g}$ state, which is an n–π^* state with excitation energy 2.28 eV whereas,[35] in bromanil, it is the $^3B_{3g}$, state which is a π–π^* state.[36] In an n–π^* transition the electron density moves away from the oxygen and the π–π^* excitation the electron density to moves away from the ring to the carbonyl groups. The higher reactivity towards hydrogen abstraction of the n–π^* triplets than the π–π^* triplets has been attributed to this redistribution of the electron density.[37]

In Table 1, the excitation energies of the triplet states of p-benzoquinone and bromanil computed at their optimized ground state geometries have been listed. Excitation energy to the lowest triplet state is 1.70 eV for p-benzoquinone. Slightly lower is the excitation energy for triplet bromanil at 1.62 eV consistent with the predictions of Shcheglova and co-workers.[36] The triplet–triplet absorption spectrum of p-benzoquinone in water has been reported by Ronfard–Haret et al. from flash photolysis studies which shows a maximum at 410 nm.[38]

Table 1. Singlet–Triplet Excitation Energies Computed at the Respective Optimized Ground State Geometry (D_{2h}) by TDDFT Calculations

	p-Benzoquinone			Bromanil		
	State	Major MOs involved	Energy eV	State	Major MOs involved	Energy eV
1	$^3B_{1g}$	$3b_{3g}\rightarrow 2b_{2g}$	1.70	$^3B_{3g}$	$4b_{1g}\rightarrow 5b_{2g}$	1.62
2	^3A_u	$4b_{2u}\rightarrow 2b_{2g}$	1.86	$^3B_{1g}$	$8b_{3g}\rightarrow 5b_{2g}$	1.74
3	$^3B_{1u}$	$2b_{3u}\rightarrow 2b_{2g}$	2.79	$^3B_{1u}$	$5b_{3u}\rightarrow 5b_{2g}$	2.13
4	$^3B_{3g}$	$1b_{1g}\rightarrow 2b_{2g}$	2.85	^3A_u	$9b_{2u}\rightarrow 5b_{2g}$	2.23
5	$^3B_{3u}$	$3b_{3g}\rightarrow 1a_u$	4.45	$^3B_{3u}$	$9b_{1u}\rightarrow 5b_{2g}$	2.35
6	$^3B_{2g}$	$4b_{2u}\rightarrow 1a_u$	4.62	$^3B_{1g}$	$7b_{3g}\rightarrow 5b_{2g}$	2.53
7	^3A_g	$1b_{2g}\rightarrow 2b_{2g}$	5.21	^3A_u	$8b_{2u}\rightarrow 5b_{2g}$	2.90
8	^3A_u	$3b_{3g}\rightarrow 3b_{3u}$	5.26	^3A_g	$4b_{2g}\rightarrow 5b_{2g}$	2.96
9	$^3B_{1g}$	$2b_{3g}\rightarrow 2b_{2g}$	5.28	$^3B_{2g}$	$10a_g\rightarrow 5b_{2g}$	3.12
10	$^3B_{1g}$	$4b_{2u}\rightarrow 3b_{1u}$	5.43	$^3B_{2u}$	$3a_u\rightarrow 5b_{2g}$	3.14

Table 2. Singlet–Triplet Excitation Energies Computed at the Respective Optimized Triplet Excited State Geometry Using TDDFT Calculations

	p-Benzoquinone (D_{2h})			Bromanil (C_{2h})		
	State	Major MOs involved	Energy eV	State	Major MOs involved	Energy eV
1	$^3B_{1g}$	$3b_{3g}\rightarrow 2b_{2g}$	1.46	^3B_g	$12b_g\rightarrow 15a_g$	1.20
2	^3A_u	$4b_{2u}\rightarrow 2b_{2g}$	1.54	^3A_u	$12a_u\rightarrow 15a_g$	1.70
3	$^3B_{1u}$	$2b_{3u}\rightarrow 2b_{2g}$	2.41	^3B_u	$14b_u\rightarrow 15a_g$	1.78
4	$^3B_{3g}$	$1b_{1g}\rightarrow 2b_{2g}$	2.53	^3B_u	$13b_u\rightarrow 15a_g$	1.98
5	$^3B_{3u}$	$3b_{3g}\rightarrow 1a_u$	4.44	^3A_u	$11a_u\rightarrow 15a_g$	2.56
6	$^3B_{2g}$	$4b_{2u}\rightarrow 1a_u$	4.54	^3A_u	$10a_u\rightarrow 15a_g$	2.80
7	^3A_g	$1b_{2g}\rightarrow 2b_{2g}$	4.77	^3B_u	$12b_u\rightarrow 15a_g$	3.22
8	$^3B_{1g}$	$2b_{3g}\rightarrow 2b_{2g}$	4.92	^3B_u	$12b_g\rightarrow 13a_u(81\%)$ $11b_g\rightarrow 13a_u(16\%)$	3.74
9	$^3B_{1u}$	$1b_{1g}\rightarrow 1a_u$	5.00	^3A_u	$12a_u\rightarrow 16a_g$	4.45

The time-resolved resonance Raman spectra of the triplet state have been recorded by Brus and co-workers[39] at nanosecond and picosecond time scales. The Raman spectrum shows four fundamental bands, with the C=C and C=O stretching modes at 1552 cm^{-1} and 1496 cm^{-1} respectively. The C–H bending mode was observed at 1163 cm^{-1} and the C–C–C + C–C stretching has been observed at 455 cm^{-1}.

In bromanil, the absorption spectrum of the triplet excited state has been recorded by us in nanosecond time scale[25] and by Hubig et al. at 3 ps.[40] The spectrum has maximum at 515 nm. The time-resolved resonance Raman spectrum in carbon tetrachloride has been reported by us recently.[24,25] Briefly, three bands were assigned to fundamentals of totally symmetric modes observed at 1561 cm^{-1}, 1396 cm^{-1} and 965 cm^{-1}. We have reported detailed DFT calculations with the optimized triplet state geometry and vibrational frequencies elsewhere.[24] The high frequency bands, viz., 1561 cm^{-1} and 1396 cm^{-1} were found to be coupled modes from the computed potential energy distribution. The band at 965 cm^{-1} was assigned to C–Br stretching combined with C–C stretching.

From the singlet–triplet excitation energies computed at the ground state geometries for both molecules, we identified the lowest triplet states for each. The geometry of this state was optimized using steady state DFT. At this optimized geometry, the singlet–triplet excitation energies were recomputed. These have been summarized in Table 2. As expected, the excitation energies are reduced as compared to the calculation at the ground state minimum.

Using the maximum of the triplet–triplet absorption spectra, we compute the expected excitation energy of the resonant triplet state for *p*-benzoquinone as 4.48 eV (1.46 eV + 3.02 eV). From Table 2, the symmetry allowed transition which matches this excitation energy is the $^3B_{3u}$. Thus the excitation from the T_1 to the T_n state corresponds to the $b_{2g} \rightarrow a_u$ transition leading to occupations of the resonant triplet state, T_n, as b_{3g} (1) a_u (1). The transition dipole moment computed for this transition is 1.38 Å and the separation of the T_1 and T_n states is predicted to be 2.98 eV. For bromanil, the T_1 to T_n transition is from the ^3B_g state to the ^3B_u state. The corresponding transition dipole moment was computed to be 0.97 Å.[25]

The parameters computed above were used in wave packet simulations of the absorption and resonance Raman spectrum. The final fits to the absorption spectra of both the molecules is shown in Fig. 1 and the resonance Raman excitation profiles of the key C=O and C–C stretching modes of both the molecules are shown in Fig. 2. The final best fit parameters are summarized in Table 3 and the experimental and simulated resonance Raman internsities are shown in Fig. 3. As seen from Table 3, the dimensionless displacements obtained for the

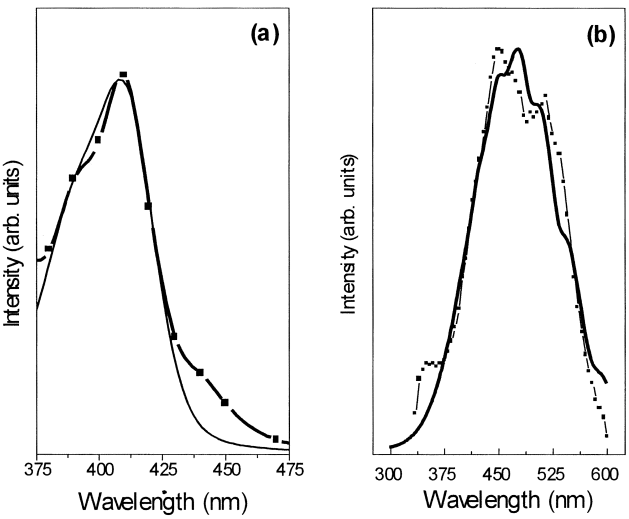

Fig. 1. Experimental (squares) and simulated (solid line) absorption spectra of the triplet excited states of (a) *p*-benzoquinone in water and (b) bromanil in carbon tetrachloride.

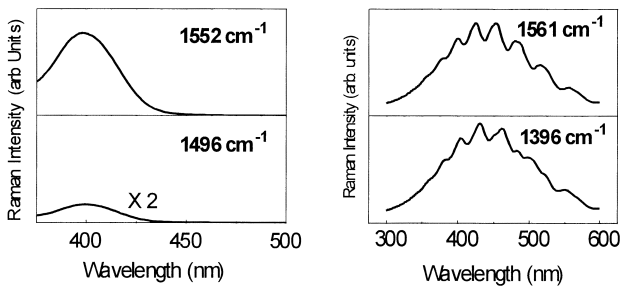

Fig. 2. Computed Raman excitation profiles of the two highest frequency modes of *p*-benzoquinone (left) and bromanil (right).

Table 3. Best-Fit Values of the Dimensionless Displacements Obtained from the Simulation

Frequency (ω_i/cm^{-1})[a)]	PED(%)[b)]	Displacement (Δ_i)	Relative intensities Expt[a)]	Calcd
	p-Benzoquinone			
	E_0 = 24185 cm^{-1}, Γ = 200 cm^{-1}, Θ = 480 cm^{-1}			
1552	C=C(59), C=O(13), δCH(15)	0.75	9.0	9.14
1496	C=O(65), C=C(14), δCH(10)	0.25	1.0	1.0
1163	δCH(90)	0.65	6.0	6.09
455	δCCC(67), C–C(23)	1.22	7.0	7.04
	Bromanil			
	E_0 = 16915 cm^{-1}, Γ = 450 cm^{-1}, Θ = 150 cm^{-1}			
1561	C=C(35), C–C(27), C=O(20)	1.51	1.0	1.0
1396	C=O(60), C=C(37)	1.61	0.87	0.88
965	C–Br(54), C–C(36)	1.53	0.58	0.56

a) Experimental frequencies and relative intensities of *p*-benzoquinone from Ref. 39.
b) PED of *p*-benzoquinone from Ref. 20.

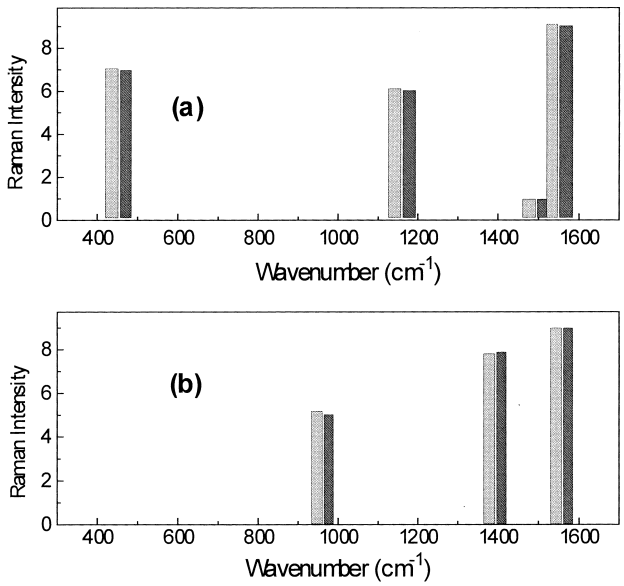

Fig. 3. Experimental (light) and simulated (dark) intensities in the time-resolved resonance Raman spectrum of the triplet states of (a) *p*-benzoquinone and (b) bromanil.

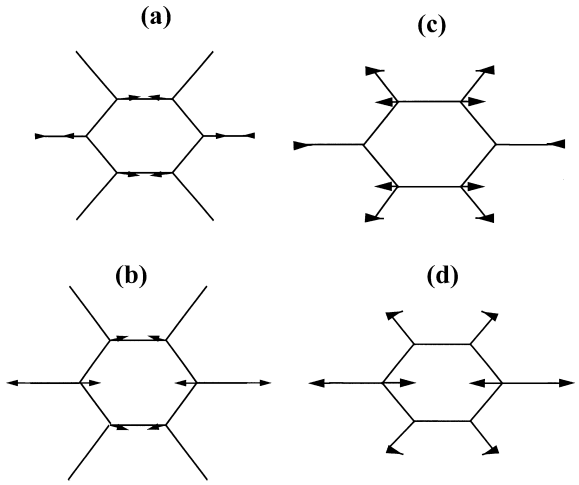

Fig. 4. Normal mode displacements of the two highest frequency modes of bromanil (a) and (b), and benzoquinone (c) and (d).

various modes of *p*-benzoquinone range from 0.25 to 1.22. The smallest displacement is observed for the C=O stretching mode. The largest displacement is observed for the lowest frequency mode at 455 cm^{-1}. Displacements along the C=C stretching and C–H bending modes are of intermediate magnitude. On the other hand, for bromanil, the dimensionless displacements for all the observed modes are similar and close to 1.5. The normal mode displacements for the two highest frequency modes of *p*-benzoquinone and bromanil are depicted in Fig. 4. From the potential energy distribution given in Table 3 and the normal modes in Fig. 4, the differences in the excited state geometry changes of the parent and substituted quinones can be inferred. The triplet state of *p*-benzoquinone, on photoexcitation, undergoes changes along the C=C bond and C–C bond as well as the C–C–H angle. The bromanil geometry however, changes along all the stretching coordinates including the C–Br stretch.

Further information on the dynamics in the excited state can be obtained from analysis of the time evolution of the absorption and Raman overlaps as has been demonstrated, e. g., in the case of stilbene.[8] In the following we discuss the time-dependent absorption and Raman overlaps of both molecules for the observed modes. In Fig. 5, the absorption overlaps of *p*-benzoquinone and bromanil are shown for each mode from 0 to 50 fs. The homogeneous damping factor is included for both the overlaps. In all the modes of the parent quinone, Fig. 5a, the absorption overlap decreases slowly. The decay of the overlap of the highest frequency band at 1552 cm^{-1} is the fastest followed by that of the band at 1163 cm^{-1}. The overlap builds up again for the 1552 cm^{-1} band first and subsequently for the band at 1163 cm^{-1}. The rebuild up of the overlap does not occur within 50 fs for the C=O stretching mode and the C–C–C

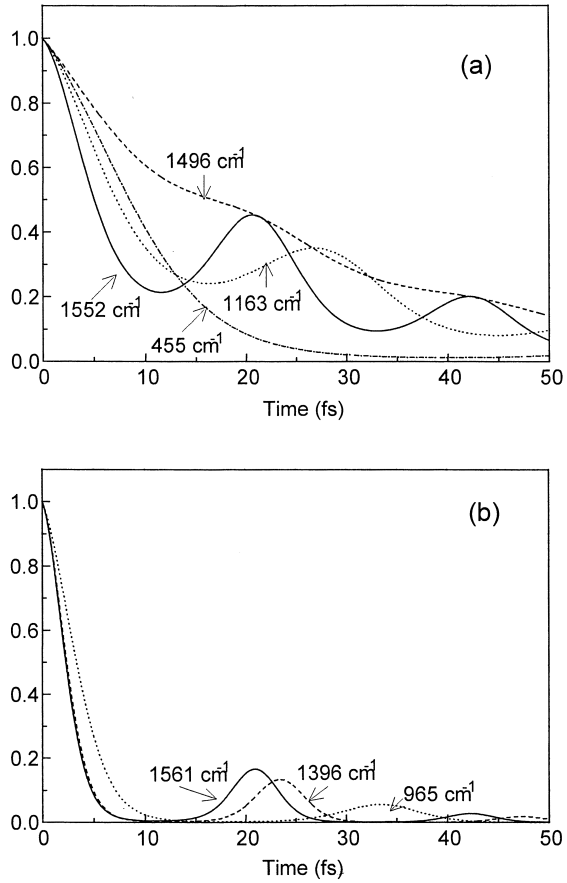

Fig. 5. Modulus of the time-dependent absorption overlap of (a) *p*-benzoquinone and (b) bromanil.

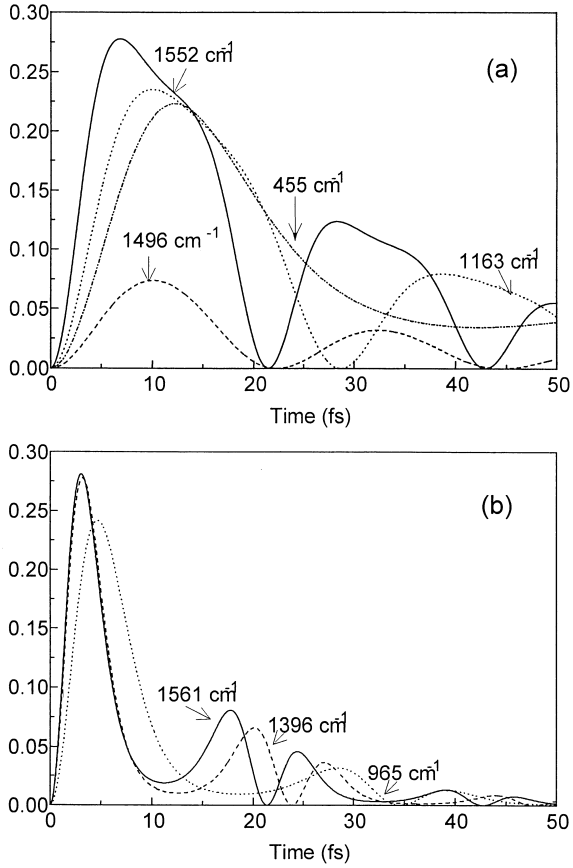

Fig. 6. Modulus of the time-dependent Raman overlap of (a) *p*-benzoquinone and (b) bromanil.

bending modes.

In contrast, the absorption overlap of bromanil, Fig. 5b, shows a rapid decay within 10 fs for all the modes. This dynamics is reflected in the observed absorption spectra of the two molecules. While absorption spectrum of the parent quinone is narrow, those of substituted quinones are much broader. Similar to the case of *p*-benzoquinone, the overlap builds again for the highest frequency mode at 1561 cm^{-1}. On the other hand, the dynamics of the mode at 1496 cm^{-1} in *p*-benzoquinone and the corresponding band at 1396 cm^{-1} in bromanil are very different. The time-dependent overlap of the 1396 cm^{-1} band of bromanil is similar to that of the band at 1561 cm^{-1}, whereas overlap of the band at 1496 cm^{-1} decays more rapidly than that of the band at 1552 cm^{-1}. Therefore, in *p*-benzoquinone, the major contribution to the absorption spectrum comes from the C=C stretching and the C–H bending modes whereas in bromanil, it is from the two highest frequency modes which are assigned to coupled C=C and C=O stretching modes. The overlap of the mode at 965 cm^{-1}, decays comparatively, rapidly. As discussed above, in bromanil, all the modes show large, similar, displacements. The large displacements in bromanil in several modes lead to a rapid movement of the wave packet away from the Franck–Condon region.

The temporal evolution of the Raman overlaps is shown in Fig. 6 from 0 to 50 fs. Since the displacements for the modes at 1552 cm^{-1} and 1163 cm^{-1} are similar, the Raman overlap in *p*-benzoquinone, reaches a maximum in these two modes at the same time. The mode at 455 cm^{-1} has lower frequency but a larger displacement and achieves mazimum overlap in the same time as the higher frequency modes due to the $\Delta^2\omega^2$ dependence of the relative Raman intensities. The Raman overlaps of the C=C and C=O coupled modes in bromanil show similar temporal evolution as expected from their nearly equal displacements. The mode at 965 cm^{-1} also reaches a maximum overlap rapidly. Thus the initial dynamics in the triplet excited state of *p*-benzoquinone is along the C=C stretching modes and the C–H bending modes while in bromanil, the dynamics is along all the stretching modes suggesting a more delocalized structure in the excited state.

Such differences in the triplet state structure, normal mode composition and the triplet state dynamics of *p*-benzoquinone and bromanil discussed here will govern the relative reactivities of the two molecules. For example, Nakano and Mori have shown that halogenated *p*-benzoquinones catalyze photoinduced reduction of the ring in octaethylporphyrin.[41] The reaction is faster in the presence of bromanil than other haloanils and does not take place in the presence of *p*-benzoquinone. The present study will help in the determination of the unequivocal mechanistic route in such reactions.

Summary

We have demonstrated application of the time-dependent theory of resonance Raman intensities to triplet states with the

well known quinone systems as examples. It is shown that time-resolved resonance Raman experimental date and density functional theoretical parameters may be used in tandem to obtain a deeper insight into the structure and dynamics of the triplet excited states. The dynamics of *p*-benzoquinone is affected significantly by substitution with bromine. The initial dynamics of bromanil is considerably faster than in *p*-benzoquinone. While the bromanil molecule becomes more delocalized subsequent to excitation from the lowest triplet state, C=C stretching and C–H bending modes dominate the dynamics in *p*-benzoquinone.

We thank Prof. J. Chandrasekhar, Indian Institute of Science, Bangalore, India and Prof. J. G. Snijders, Theoretical Chemistry, Materials Science Centre, Rijksuniversiteit Groningen, Groningen, The Netherlands, for discussion. We thank the Department of Science and Technology (DST), India and the Council for Scientific and Industrial Research (CSIR), India for financial support.

References

1 S. Lee and E. J. Heller, *J. Chem. Phys.*, **71**, 4777 (1979).

2 R. Mathies, "Chemical and Biochemical Applications of Lasers," ed by C. B. Moore, Academic Press, New York (1979), Vol. IV, p. 55.

3 E. J. Heller, *Acc. Chem. Res.*, **14**, 368 (1981).

4 A. B. Myers and R. A. Mathies, "Biochemical Applications of Raman Spectroscopy," ed by T. G. Spiro, Wiley, New York (1987), Vol. 2, p. 1.

5 A. B. Myers, *J. Raman Spectrosc.*, **28**, 389 (1997); A. B. Myers, *Chem. Rev.*, **96**, 911 (1996); A. B. Myers, "Laser Techniques in Chemistry," Techniques of Chemistry Series, ed by Anne B. Myers and T. R. Rizzo, John Wiley and Sons., Inc. (1995), Vol. XXIII, PP. 325–384.

6 J. L. Zink and K.-S. K. Shin, *Adv. Photochem.*, **16**, 119 (1991).

7 N. Biswas and S. Umapathy, *Curr. Sci.*, **74**, 328 (1998).

8 A. B. Myers and R. A. Mathies, *J. Chem. Phys.*, **81**, 1552 (1984).

9 J. Rodier and A. B. Myers, *J. Am. Chem. Soc.*, **115**, 10791 (1993).

10 N. Biswas and S. Umapathy, *J. Chem. Phys.*, **107**, 7849 (1997).

11 N. Biswas and S. Umapathy, *Chem. Phys. Lett.*, **236**, 24 (1995).

12 N. Biswas and S. Umapathy, *Chem. Phys. Lett.*, **294**, 181 (1998).

13 A. P. Esposito, C. E. Foster, R. A. Beckman, and P. J. Reid, *J. Phys. Chem. A*, **101**, 5309 (1997).

14 L. M. Markham and B. S. Hudson, *J. Phys. Chem.*, **100**, 2731 (1996).

15 L. M. Markham, L. C. Mayne, B. S. Hudson, and M. Z. Zgierski, *J. Phys. Chem.*, **97**, 10319 (1993); B. S. Hudson and L. M. Markham, *J. Raman Spectrosc.*, **29**, 489 (1998).

16 T. Keszthelyi, G. Balakrishnan, R. Wilbrandt, W. A. Yee, and F. Negri, *J. Phys. Chem. A*, **104**, 9121 (2000); A. M. Brouwer, J. M. Zwier, C. Svendsen, O. S. Mortensen, F. W. Langkilde, and R. Wilbrandt, *J. Am. Chem. Soc.*, **120**, 3748 (1998); A. M. Brouwer, C. Svendsen, O. S. Mortensen, and R. Wilbrandt, *J. Raman Spectrosc.*, **29**, 439 (1998).

17 F. W. Langkilde, R. Wilbrandt, A. M. Brouwer, F. Negri, and G. Orlandi, *J. Phys. Chem.*, **98**, 2254 (1994); F. W. Langkilde, R. Wilbrandt, S. Moller, A. M. Brouwer, F. Negri, and G. Orlandi, *J. Phys. Chem.*, **95**, 6884 (1991); F. Negri, G. Orlandi, A. M. Brouwer, F. W. Langkilde, S. Moller, and R. Wilbrandt, *J. Phys. Chem.*, **95**, 6895 (1991); F. Negri, G. Orlandi, A. M. Brouwer, F. W. Langkilde, and R. Wilbrandt, *J. Chem. Phys.*, **90**, 5944 (1989).

18 S. E. Boesch and R. A. Wheeler, *J. Phys. Chem.*, **99**, 8125 (1995); S. E. Boesch and R. A. Wheeler, *J. Phys. Chem.*, **101**, 8351 (1997).

19 D. Pan, L. C. T. Shoute, and D. L. Phillips, *J. Phys. Chem. A*, **103**, 6851 (1999); D. Pan, L. C. T. Shoute, and D. L. Phillips, *J. Phys. Chem. A*, **104**, 4140 (2000).

20 P. Mohandas and S. Umapathy, *J. Phys. Chem. A*, **101**, 4449 (1997).

21 N. Biswas and S. Umapathy, *J. Phys. Chem. A*, **101**, 5555 (1997); N. Biswas and S. Umapathy, *J. Phys. Chem.*, **104**, 2734 (2000).

22 G. Balakrishnan, P. Mohandas, and S. Umapathy, *Spectrochim. Acta A*, **53**, 153 (1997).

23 G. Balakrishnan, P. Mohandas, and S. Umapathy, *J. Phys. Chem. A*, **105**, 7778 (2001).

24 M. Puranik, J. Chandrasekhar, J. G. Snijders, and S. Umapathy, *J. Phys. Chem. A*, **105**, 10562 (2001).

25 M. Puranik, S. Umapathy, J. G. Snijders, and J. Chandrasekhar, *J. Chem. Phys.*, **115**, 6106 (2001).

26 S. J. A. van Gisbergen, J. G. Snijders, and E. J. Baerends, *Comput. Phys. Commun.*, **118**, 119 (1999).

27 A. Rosa, E. J. Baerends, S J. A. van Gisbergen, E. van Lenthe, and J. G. Snijders, *J. Am. Chem. Soc.*, **121**, 10356, (1999); S. J. A. van Gisbergen, J. A. Groeneveld, A. Rosa, J. G. Snijders, and E. J. Baerends, *J. Phys. Chem. A*, **103**, 6835 (1999); S. J. A. van Gisbergen, J. G. Snijders, and E. J. Baerends, *Phys. Rev. Lett.*, **78**, 3097 (1997).

28 G. Balakrishnan, P. Mohandas, and S. Umapathy, *J. Phys. Chem.*, **100**, 16472 (1996).

29 a) ADF 1999, E. J. Baerends, A. Bérces, C. Bo, P. M. Boerrigter, L. Cavallo, L. Deng, R. M. Dickson, D. E. Ellis, L. Fan, T. H. Fischer, C. Fonseca Guerra, S. J. A. van Gisbergen, J. A. Groenevels, O. V. Gritsenko, F. E. Harris, P. van den Hoek, H. Jacobsen, G. van Kessel, F. Kootstra, E. van Lenthe, V. P. Osinga, P. H. T. Philipsen, D. Post, C. C. Pye, W. Ravenek, P. Ros, P. R. T. Schipper, G. Schreckenbach, J. G. Snijders, M. Sola, D. Swerhone, G. te Velde, P. Vernooijs, L. Versluis, O. Visser, E. van Wezenbeek, G. Wiesenekker, S. K. Wolff, T. K. Woo, T. Ziegler. b) E. J. Baerends, D. E. Ellis, and P. Ros, *Chem. Phys.*, **2**, 41 (1973); c) L. Versluis and T. Ziegler, *J. Chem. Phys.*, **322**, 88 (1988), d) G. te Velde and E. J. Baerends, *J. Comput. Phys.*, **99**, 84 (1992), e) C. F. Guerra, J. G. Snijders, G. te Velde, and E. J. Baerends, *Theor. Chem. Acc.*, **99**, 391 (1998).

30 S. H. Vosko, L. Wilk, and M. Nusair, *Can. J. Phys.*, **58**, 1200 (1980).

31 A. D. Becke, *Phys. Rev. A*, **38**, 3098 (1988).

32 C. Lee. W. Yang, and R. G. Parr, *Phys. Rev., B*, **37**, 785 (1988).

33 D. J. Tannor and E. J. Heller, *J. Chem. Phys.*, **77**, 202 (1982).

34 E. J. Heller, R. L. Sundberg, and D. Tannor, *J. Phys. Chem.*, **86**, 1822 (1982).

35 M. Koyanagi, Y. Kogo, and Y. Kanda, *J. Mol. Spectrosc.*,

34, 450 (1970).

36 N. A. Shcheglova, D. N. Shigorin, G. G. Yakobson, and L. Sh. Tushishvili. *Russ. J. Phys. Chem.*, **43**, 1112 (1969).

37 P. J. Wagner, in "Topics in Current Chemistry", ed by A. Davison, M. J. S. Dewer, K. Hafner, E. Heilbronner, U. Hofmann, J. M. Lehn, N. Niedenzu, K. I. Schäfer, and G. Wittig, Springer-Verlag, Berlin (1976), Vol. 66, p. 1.

38 J. Ronfard-Haret, R. V. Bensasson, and E. Amouyal, *J. Chem. Soc., Faraday Trans 1*, **76**, 2432 (1980).

39 S. M. Beck and L. E. Brus, *J. Am. Chem. Soc.*, **104**, 4789 (1982); S. M. Beck and L. E. Brus, *J. Am. Chem. Soc.*, **104**, 1103 (1982); R. Rossetti, S. M. Beck and L. E. Brus, *J. Phys. Chem.*, **87**, 3058 (1983); R. Rossetti and L. E. Brus, *J. Am. Chem. Soc.*, **108**, 4718 (1986).

40 S. M. Hubig, T. M. Bockman, and J. K. Kochi, *J. Am. Chem. Soc.*, **119**, 2926 (1997).

41 T. Nakano and Y. Mori, *Bull. Chem. Soc. Jpn.*, **67**, 2627 (1994).